Catalysis Today 156 (2010) 58–64

Contents lists available at ScienceDirect

Catalysis Today

journal homepage: www.elsevier.com/locate/cattod

Liquid fuels from Fischer–Tropsch wax hydrocracking: Isomer distribution

Simone Gamba [a,*], Laura A. Pellegrini [a], Vincenzo Calemma [b], Chiara Gambaro [b]

[a] *Dipartimento di Chimica, Materiali e Ingegneria Chimica "G. Natta", Politecnico di Milano, Piazza Leonardo da Vinci 32, I-20133 Milano, Italy*
[b] *Eni S.p.A., Divisione Refining & Marketing, Centro Ricerche di San Donato Milanese, Via Felice Maritano 26, I-20097 San Donato Milanese, Milano, Italy*

ARTICLE INFO

Article history:
Available online 16 February 2010

Keywords:
Fischer–Tropsch
Hydrocracking
Mono-branched isomers
Multi-branched isomers
Synthetic fuels
Wax

ABSTRACT

Considering the current need of low emission fuels for the automotive market and the need of renewable fuels that will emerge in the very next future, Fischer–Tropsch (FT) based technologies should be considered a valid option to accomplish both low emission and renewable fuel production targets. A hydrocracking step is necessary for obtaining high quality fuels from FT wax. Isomerisation is an important reaction that takes place during the hydroconversion process. The amount and the type of the isomers in the produced fuels heavily influence both cold flow properties and cetane number. In this paper the results of a detailed method of analysis which allows the distinction between mono-branched and multi-branched isomers in fuels obtained from an FT wax hydrocracking process, are presented and discussed. In particular the influence of the operating conditions and the wax conversion on the isomer distribution is pointed out.

1. Introduction

The increasing attention to environmental issues and the current legislation represent a huge driving force in developing processes to obtain "cleaner" fuels and fuels from renewable sources. Both the European Union and the United States are calling for a restriction of the emission standards for heavy-duty diesel engines and an increased production of renewable fuels [1].

In the light of these considerations Fischer–Tropsch (FT) based technologies assume a particular relevance since, as demonstrated by recent studies [2,3], FT-derived diesel has excellent combustion properties and leads to a reduction of emissions. Moreover feedstocks for an FT-based process can vary from fossil sources (natural gas or coal) to renewable biomass. There are already commercial applications of CTL (coal to liquids) and GTL (gas to liquids) processes by Sasol, PetroSA, and Shell [4] while commercial biofuels production via gasification of biomass has not taken place yet [5]. In any case, since the production of FT synfuels from biomass can play an important role in the future as a source of carbon neutral fuels for CO_2 emission containment [4], different studies have been conducted in recent years in order to investigate the feasibility of an integrated biomass gasification and Fischer–Tropsch system [6–8]. Synthesis of second-generation biofuels (which have a much higher environmental efficiency compared to the first-generation fuels like biodiesel [7]) via FT-based technology is starting to emerge as a valid option to obtain renewable fuels [9–13].

In most cases, FT products (characterised by a wide range of molecular weights, whose distribution can be described by the Anderson–Schulz–Flory model [14]) need to be upgraded in order to become suitable as transportation fuel. In particular, the heaviest products (characterised by a boiling point higher than 370 °C) must be cracked into the middle distillate (MD) range (i.e., 150–370 °C cut) and n-paraffins must be isomerised to improve fuel cold flow properties. The best way to reach the desired fuel yield and quality is to subject the FT effluent to a hydrocracking step over a proper bifunctional catalyst [15–24].

Isomers have a great influence on both cold flow properties and cetane number [2,25,26] and thus controlling the amount of isomers and the degree of branching plays a key role in conducting the hydrocracking process.

In this paper attention is focused on the distribution of isomers in the naphtha and MD cuts obtained from the three-phase hydrocracking of FT wax [27], in the light of experimental data obtained by a detailed method of analysis able to distinguish between mono-branched and multi-branched paraffins. The influence of the operating conditions (temperature, pressure, H_2/wax inlet mass ratio and weight hourly space velocity—WHSV) and thus of the wax conversion on the extent of the isomerisation reaction will be investigated.

2. Experimental

The experimental data were collected on the hydrocracking unit placed in Eni's laboratories. The unit is equipped with a down-

---

* Corresponding author. Tel.: +39 02 2399 3237; fax: +39 02 7063 8173.
E-mail addresses: simone.gamba@mail.polimi.it (S. Gamba), laura.pellegrini@polimi.it (L.A. Pellegrini), vincenzo.calemma@eni.it (V. Calemma), chiara.gambaro@eni.it (C. Gambaro).

0920-5861/$ – see front matter © 2010 Elsevier B.V. All rights reserved.
doi:10.1016/j.cattod.2010.01.009

flow trickle bed reactor (ID = 16 mm), loaded with 9 g of powdered fresh catalyst. The catalyst is a typical bifunctional system, made of Pt particles dispersed on an amorphous silico-alumina matrix. The extruded particles are crushed and sieved in the range of 20–40 mesh (average particle size (D_p) = 0.625 mm, catalytic bed height (H_b) = 86 mm) in order to approximate the plug flow behaviour. The empirical correlations presented in literature [28] for ideal behaviour of tubular reactors are:

$$\frac{\mathrm{ID}}{D_p} > 25 \tag{1}$$

to minimize by-pass, and

$$\frac{H_b}{D_p} > 100 \tag{2}$$

to minimize back-mixing.

Both relations are satisfied for the system used.

The catalyst was activated in situ by reduction with pure H_2 at high pressure and temperature, according to standard procedure.

The effect of the operating conditions on activity and selectivity was determined by planning the experiments according to a Central Composite Design [27]. The range of the operating conditions was: temperature = 616.15–648.15 K; pressure = 35–60 bar; H_2/wax = 0.06–0.15 kg/kg; WHSV = 1–3 h^{-1}. The feedstock used in this study was a paraffinic FT wax (olefins and alcohols had previously been removed) whose mass chain length distribution is reported in Fig. 1 (the molar chain length distribution has already been reported [29]).

A preliminary data set has already been used for the development of different versions of a hydrocracking model [29–34].

2.1. Product analysis

The gaseous fraction of products was analysed by a GC HP 5890 II equipped with an FID (Flame Ionization Detector) and an automatic sampling loop. The column used was an HP PONA crosslinked methyl siloxane, 50 m (L) × 0.2 mm (ID) × 0.5 μm (film thickness). Temperature programming of the oven was 7.5 min at 35 °C then up to 70 °C with a linear ramp rate of 3 °C min^{-1}, subsequently up to 220 °C at 7.5 °C min^{-1} and maintaining the final temperature for 45 min.

A first liquid product analysis (able to obtain the liquid phase composition as the weight percentage of the normal and the iso-paraffin lump of each single aliphatic chain present) was carried out with a GC HP-5890 II equipped with an on column injection system, an Electronic Pressure Control, and an FID. The column used was an SPB-1 (Supelco) 15 m (L) × 0.53 mm (ID) × 0.1 μm (film thickness). Temperature programming of the oven was: 1 min at 0 °C then up to 315 °C with a linear ramp rate of 5 °C min^{-1} and a holding time of 37 min at the final temperature. Temperature programming of the injector was 1 min at 50 °C then up to 330 °C with a linear ramp rate of 5 °C min^{-1} and a holding time of 37 min at the final temperature.

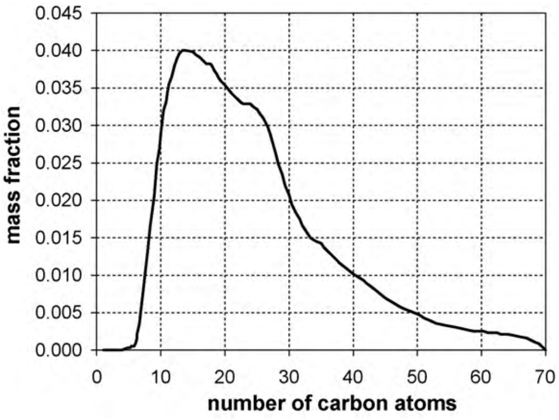

Fig. 1. Composition of the wax (n-paraffin) mixture used for the experimental tests.

For both analyses the carrier used was helium.

The overall composition of hydrocracking products was obtained by merging together the results of liquid and gas product analyses according to their weight fraction.

The liquid fraction was also analysed by a second method (reported below), characterised by a higher resolution of the lighter components, which allowed to distinguish among the different classes of isomers such as mono-, di-, and tri-branched paraffins for chain lengths lower than 25 carbon atoms.

In this case the liquid products were analysed by a GC HP 6890 Plus T equipped with Electronic Pressure Control and FID, supplied with a switching system (G2855B Deans Switching System) which allowed the fraction C_{30-} of the liquid sample to be sent to the column used for the separation while the heavier fraction was vented out. The column was an HP-5 high speed 5% phenyl methyl siloxane, 50 m (L) × 0.2 mm (ID) × 0.5 μm (film thickness). The carrier gas was hydrogen.

Temperature programming of the oven was: 3 min at 35 °C then up to 180 °C with a linear ramp rate of 2 °C min^{-1}, maintaining 180 °C for 75 min then up to 220 °C at a speed of 1.5 °C min^{-1}, keeping 220 °C for 102 min then up to 250 °C at a speed of 1.2 °C min^{-1}. Finally maintaining 250 °C for 71 min.

Identification of GC peaks was accomplished by GC–MS analysis and, when possible, by the addition of pure compounds to the mixture of products. In this case the overall carbon distribution was obtained merging together the results of the three analyses (gas, liquid high resolution method – C_{23-} – and liquid low resolution method) according to their weight fractions.

Fig. 2 reports two different GC analysis results (one obtained from the low resolution method (Fig. 2a) and the other obtained from the high resolution method (Fig. 2b)) for the same sample in the C_{15}–C_{17} product range. The enhancement in the resolution is clear but the second method of analysis is more time consuming. Observing Fig. 2b it is possible to note how some multi-branched isomers with 17 and 18 carbon atoms have a retention time (i.e., a boiling point) lower than nC_{16} and nC_{17} respectively. Such a behaviour has already been observed (albeit on an average base) in a study for the thermodynamic characterisation of paraffin lumps in order to obtain critical parameters [35]. Thus, the high resolution method allows the correct identification of GC peaks of multi-branched isomers (it should be pointed out that, for high degrees of conversion as well, tri-branched isomers, i.e., the isomers with the lowest boiling point, occur solely in traces [25,36]).

3. Results and discussion

Below, the effect of the operating conditions on the extent of the isomerisation reaction for the C_{23-} fraction will be discussed. It needs to be highlighted that the global system behaviour is determined by both isomerisation and cracking reactions since experimental data refer to high conversion conditions as well. The conversion refers to the wax (C_{22+}) and it is defined as:

$$\xi_{C_{22+}} = \frac{\omega_{C_{22+}\,in} - \omega_{C_{22+}\,out}}{\omega_{C_{22+}\,in}} \times 100 \tag{3}$$

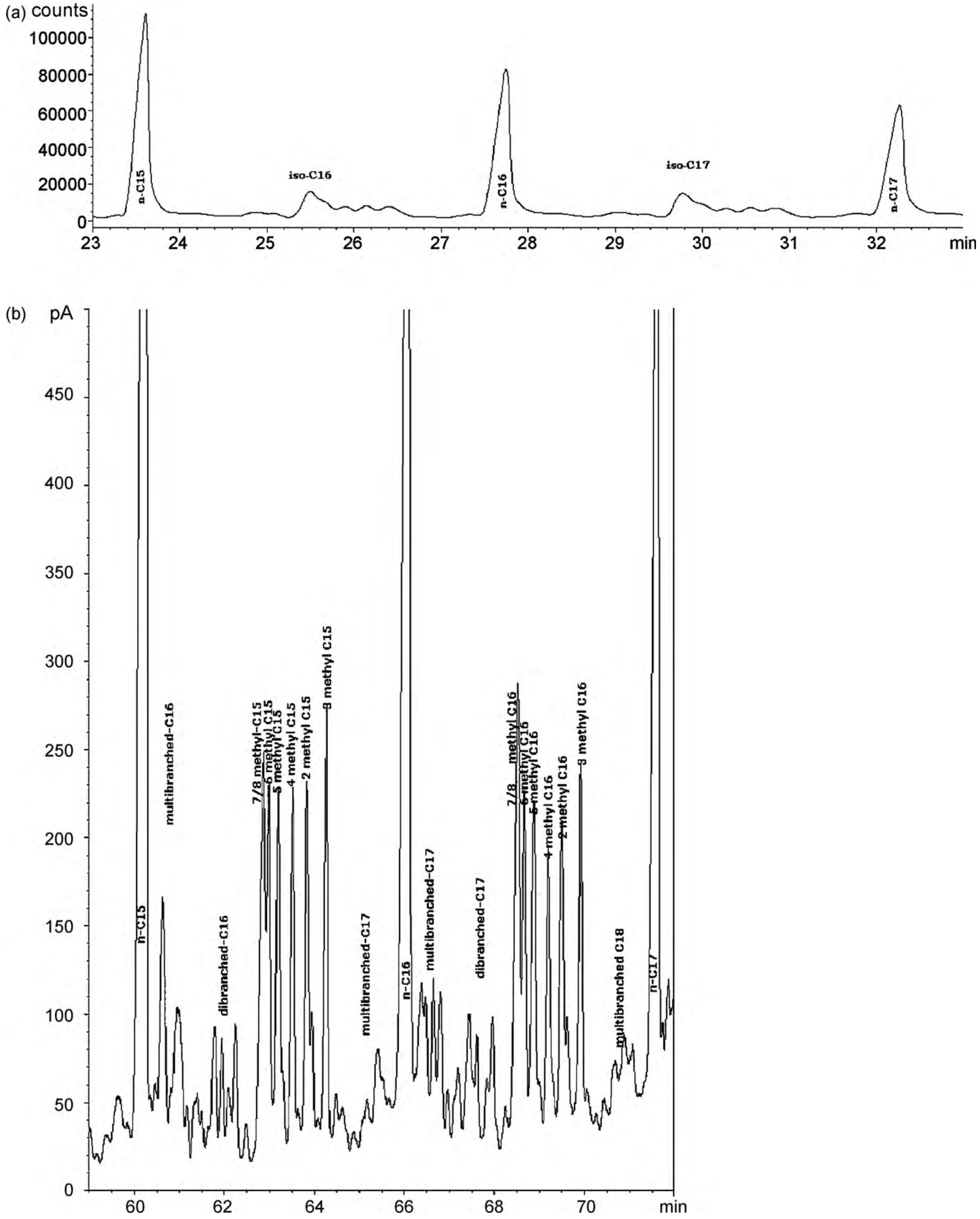

Fig. 2. GC analysis results for a given sample: (a) low resolution method and (b) high resolution method.

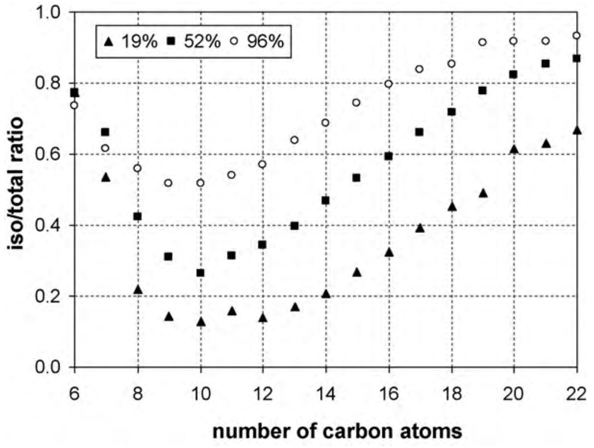

Fig. 3. Iso/total ratio for runs at three different levels of conversion (19%, 52% and 96%).

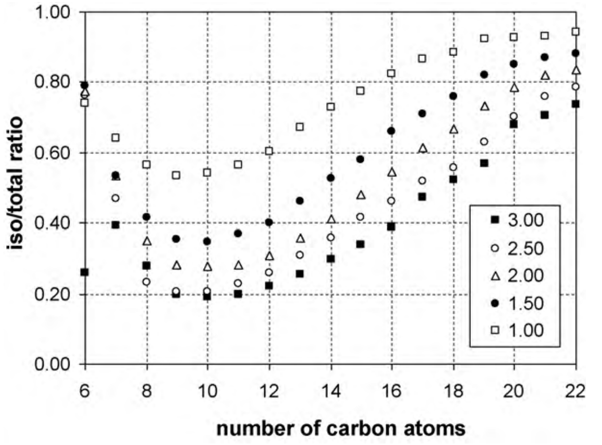

Fig. 5. WHSV effect on the iso/total ratio: the values of WHSV (h^{-1}) are indicated while the other operating conditions are: $T = 632.15$ K, $P = 47.5$ bar, H_2/waxes = 0.105 kg/kg.

3.1. Total isomer percentage

The isomerisation degree of the hydrocracking product mixture is defined as the ratio:

$$\text{iso/total}_{n_C} = \frac{\omega_{iso,n_C}}{\omega_{iso,n_C} + \omega_{normal,n_C}} \quad (4)$$

The isomer fraction is a function of chain length (n_C): data calculated for experimental runs at different levels of conversion are reported in Fig. 3. Regardless of the level of conversion, the mass ratio of branched alkanes (Eq. (4)) follows the same trend in relation to the number of carbon atoms. In particular, the iso/total ratio exhibits a minimum around C_{10}–C_{11}. This can be explained observing the feed composition and taking into account the individual reactivity of each paraffin. In the feed stream the nC_8–nC_{14} fraction has a relatively high concentration and the maximum value in the chain length distribution in the feed corresponds to a minimum value in the iso/total ratio. In order to understand this behaviour, it is worth pointing out that: (1) in the experimental runs we are considering reaction occurs in both vapour (especially for runs at higher conversion) and liquid phase [33]; (2) heavier hydrocarbons show a higher intrinsic reactivity than lighter hydrocarbons and the difference in global reactivity from the vapour phase is enhanced by the differences in physisorption [37]; (3) in the liquid phase the heaviest hydrocarbons have a molar fraction higher than the lightest ones and this last behaviour can explain the already observed effect of H_2/wax ratio on the global conversion [29]. Thus the lower reactivity and the higher feed concentration of the nC_8–nC_{14} fraction, if compared with the nC_{15}–nC_{22} fraction, lead to a decreased iso/total ratio of the C_8–C_{14} fraction. Increasing the conversion the iso/total ratio increases as expected for both a more pronounced isomerisation reaction and an increased quantity of cracking products from the C_{22+} fraction. The widely accepted mechanism for a hydrocracking process is made up of successive isomerisations (i.e., from normal to mono-branched paraffins, from mono-branched to di-branched paraffins and so on) followed by the cracking of branching products [38,39]. Martens et al. [40] proposed four different types of cracking modes: those starting from a tri-branched or a di-branched alkane (A, B1 or B2) are faster than the mechanism starting from a mono-branched alkane (C) and give as product at least one mono-branched paraffin. Thus also the cracking of the heaviest hydrocarbons contributes to increase the iso/total ratio of the C_{23-} fraction.

In order to point out the influence of the operating conditions on the isomerisation reaction the mass ratio of branched alkanes (Eq. (4)) is reported in Figs. 4–7 for test runs characterised by the same operating conditions but the analysed variable.

The effect of temperature, WHSV and pressure on the iso/total ratio is the same effect already observed on the wax conversion

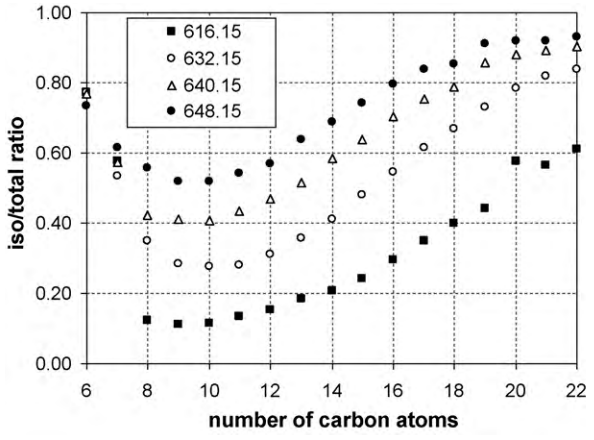

Fig. 4. Temperature effect on the iso/total ratio: the values of temperature (K) are indicated while the other operating conditions are: $P = 47.5$ bar, H_2/waxes = 0.105 kg/kg, WHSV = 2 h^{-1}.

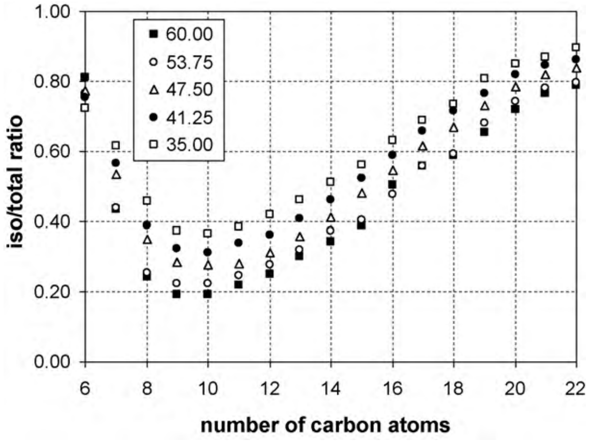

Fig. 6. Pressure effect on the iso/total ratio: the values of pressure (bar) are indicated while the other operating conditions are: $T = 632.15$ K, H_2/waxes = 0.105 kg/kg, WHSV = 2 h^{-1}.

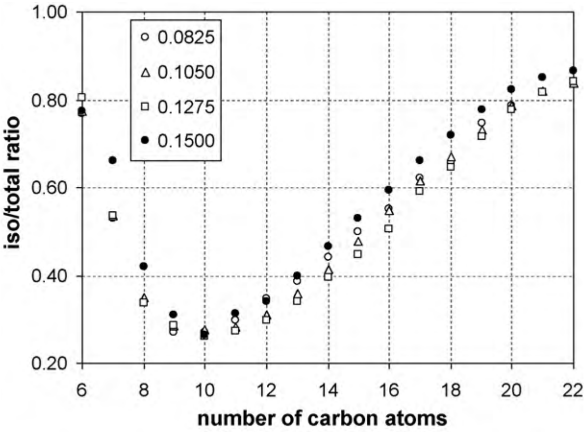

Fig. 7. Hydrogen to wax ratio effect on the iso/total ratio: the values of H_2/wax ratio (kg/kg) are indicated while the other operating conditions are: $T = 632.15$ K, $P = 47.5$ bar, WHSV = 2 h^{-1}.

[29]: the higher the conversion, the higher the iso/total ratio. It has to be pointed out that the above-mentioned operating conditions affect both the wax conversion and the reactivity of the C_{23-} fraction.

A different behaviour is encountered for the H_2/wax ratio: the iso/total ratio for the C_{23-} fraction is practically independent of the H_2/wax ratio. First of all, this variable is the one that has the lowest impact on the wax conversion [29]. Moreover increasing the H_2/wax ratio the liquid phase becomes richer in the heaviest hydrocarbons (C_{22+}) but the stripping effect of the hydrogen leads to a depletion of the lightest hydrocarbons in the liquid phase itself (that is more reactive than the vapour phase [18]). Thus the increased conversion of the wax fraction (C_{22+}), due to a thermodynamic effect, is not accompanied by an effect on the reactivity of the C_{23-} fraction. This could be the reason why the H_2/wax ratio, that has a limited effect on the conversion, has practically no effect on the iso/total ratio of the lightest hydrocarbons.

3.2. Multi-branched and mono-branched isomer distribution

Fig. 8 shows the product weight fractions of normal, mono-branched, and multi-branched isomers for four paraffins (C_8, C_{12}, C_{17}, and C_{22}) as a function of the wax (C_{22+}) conversion (i.e., cracking severity). Details about the type of side chains usually formed during a hydroconversion process have already been reported [2,36].

C_8 paraffin (Fig. 8a) is a typical example for a relatively light paraffin in the naphtha cut (C_5–C_9) while C_{12} (Fig. 8b) is representative of the kerosene cut (C_{10}–C_{14}). They show a relatively similar behaviour: the normal paraffin weight fraction is practically insensible to the wax conversion value, while the concentrations of mono-branched and multi-branched paraffins increase in relation to the wax conversion. Moreover the mono-branched isomer weight percentage is always greater than the multi-branched isomer one. Thus the rate of formation of the n-paraffin by means of the cracking of the heaviest hydrocarbons and the net rate of isomerisation are substantially equal. However C_{12} fraction undergoes appreciable isomerisation for severe operating conditions. The formation of branched C_8 and C_{12} paraffins is due to the cracking of heavier hydrocarbons. Mono-branched isomer are formed in a higher

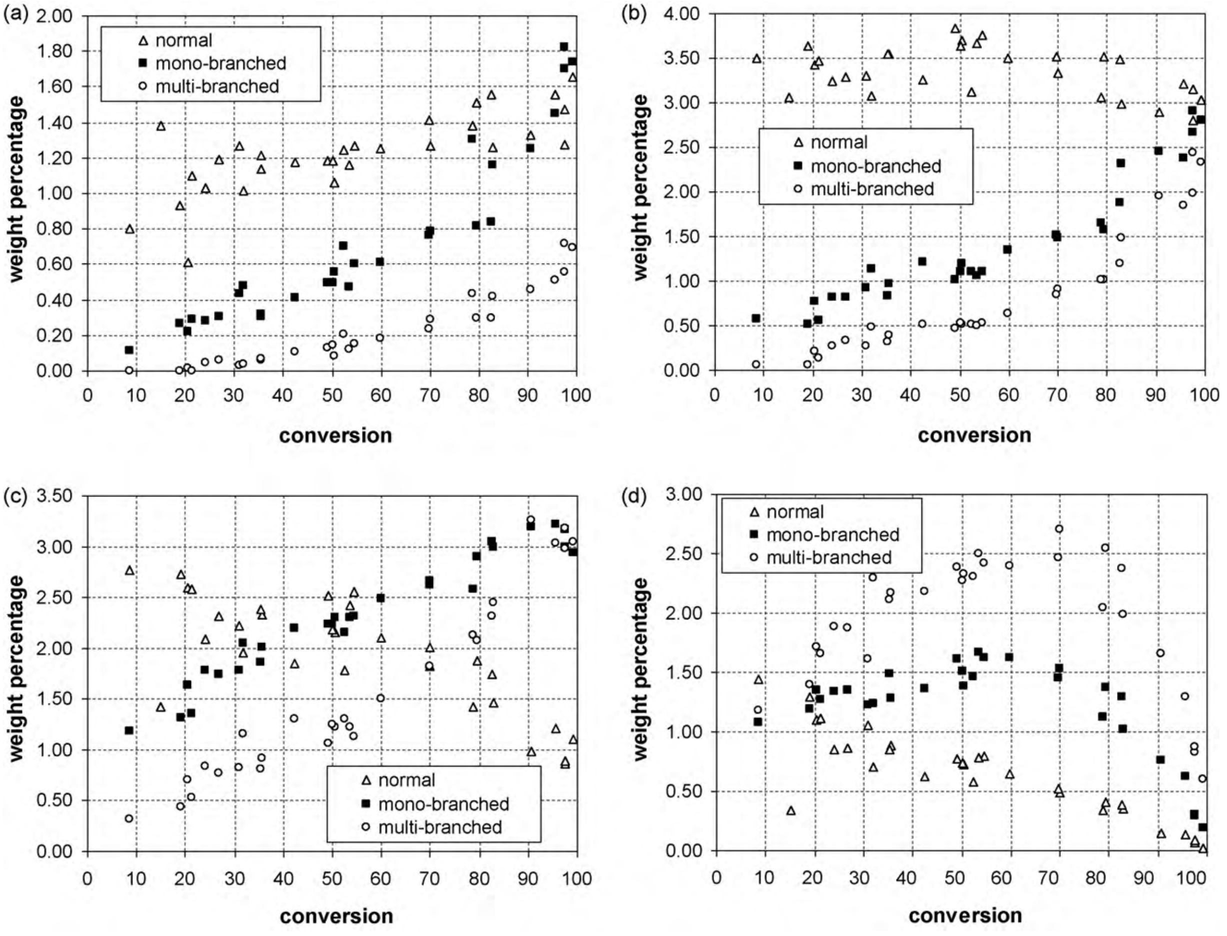

Fig. 8. Isomer weight percentage as a function of wax conversion for four paraffins: (a) C_8 paraffin; (b) C_{12} paraffin; (c) C_{17} paraffin; (d) C_{22} paraffin.

amount: A cracking mechanism on α,α,γ-tri-branched isomers and B1 and B2 cracking mechanisms on α,α- or α,γ-di-branched isomers give rise to at least one mono-branched product [40] while di-branched products can be formed only by a slow C cracking mechanism or a B1 or B2 cracking mechanism on some tri-branched isomers. It was found in literature [41] that B1, B2 and C cracking mechanisms on tri-branched isomers different from the α,α,γ-type are of little importance and the alkyl shift reaction (which can lead to structures that can be cracked by an A-type β-scission) is a faster reaction. Subsequent isomerisation of mono-branched isomers becomes important only for severe operating conditions (i.e., high wax conversion). Cracking does not affect the C_8 and C_{12} paraffin concentrations even for high wax conversion values: the rate of formation is greater than the rate of consumption.

C_{17} paraffin (Fig. 8c) is representative of the gas oil cut (C_{15}–C_{22}) and shows a cracking behaviour very similar to that of C_8 and C_{12}. Instead a different situation occurs in this case for the isomerisation. C_{17} n-paraffin is affected by a positive net rate of isomerisation (greater than the rate of formation of nC_{17} by means of cracking of heavier hydrocarbons) over the whole wax conversion range. The isomerisation from mono-branched to multi-branched isomers is not negligible and for the most severe operating conditions the weight fraction of multi-branched isomers becomes greater than that of mono-branched isomers (which shows a maximum-like behaviour). This is coherent with a mechanism of subsequent isomerisation steps. It should be outlined that by a comparison with previously worked out values of "lumped" equilibrium constants for paraffin isomerisation (even though calculated for the gas phase only) [42] and by taking into account the influence of the temperature on the isomer amount showed in Section 3.1, the system has been found to be far from the equilibrium conditions and the isomerisation reactions are kinetically and not thermodynamically controlled.

C_{22} (Fig. 8d) is the heaviest paraffin in the gas oil range and shows a behaviour that can be representative of compounds in the wax fraction (C_{22+}) as well. It is evident how this paraffin is affected by both isomerisation and cracking. Isomerisation of nC_{22} has always a positive net rate and the nC_{22} weight percentage in the product stream decreases almost linearly in relation to the wax conversion. Both mono-branched and multi-branched isomers show a maximum-like behaviour which indicates that, at high conversions: (1) mono-branched isomers are affected by the subsequent isomerisation to multi-branched paraffins and by cracking (even if this last one should not be so important since mono-branched isomers can undergo cracking only by means of a slow C mechanism [40]); (2) multi-branched isomers are affected by cracking reactions while the reverse isomerisation seems to be negligible since for heavy hydrocarbons the lumped equilibrium constants are very high [42]. The concentration of multi-branched isomers is always greater than that of mono-branched ones, confirming the very favoured second step of the isomerisation reaction. Finally it needs to be highlighted that, form previous studies [33], the gas oil cut behaviour has been found to be more similar to that of the C_{17} rather than to that of the C_{22}.

In order to complete the analysis of the influence of the wax conversion on the single n-paraffin isomerisation, Fig. 9 shows the weight percentage of mono- and multi-branched isomers of each hydrocarbon in the C_6–C_{22} range in the product stream for two tests, one characterised by low wax conversion and the other one characterised by high wax conversion. It is clear how for the low conversion test, the weight fraction of branched paraffins increases with the number of carbon atoms due to the intrinsic higher reactivity of heavier hydrocarbons and the thermodynamic effect of the VLE [29]. However since the system is not under equilibrium conditions and considering the feed concentration of each single alkane, the concentration does not increase so sharply in relation to the number of carbon atoms [42]. Moreover the values of weight fractions of light paraffin isomers (whose second isomerisation is negligible) are consistent with a mechanism of subsequent isomerisations. Observing the high conversion test, it is possible to note how the isomer concentration does not increase continuously with the number of carbon atoms but sharply decreases starting from C_{18}. This can be readily explained by considering the cracking reaction that starts to affect relatively light hydrocarbons as well and a more favoured second step of isomerisation.

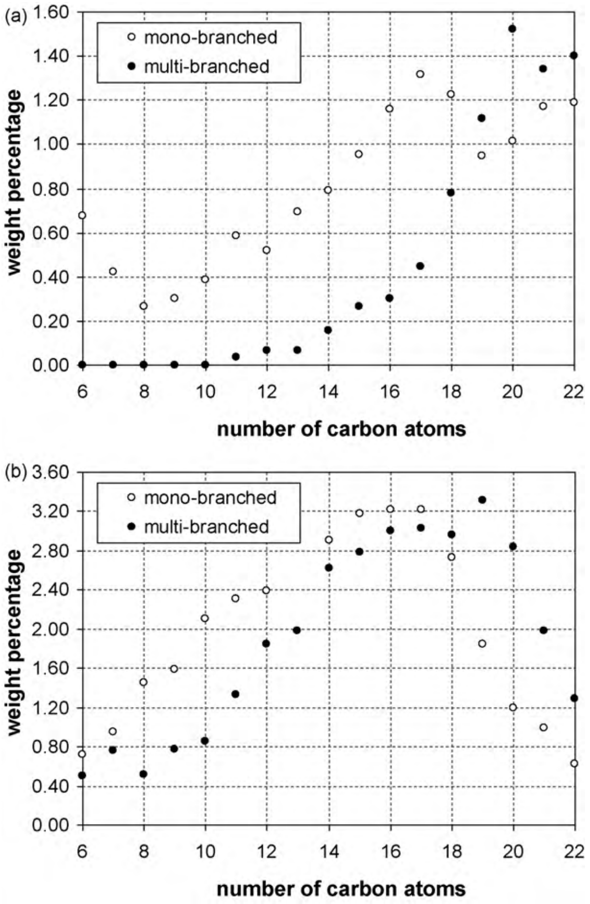

Fig. 9. Mono-branched and multi-branched isomer weight percentage in the product stream of each paraffin in the C_6–C_{22} range: (a) 19% wax conversion test run and (b) 96% wax conversion test run.

4. Conclusions

In this paper experimental data about the isomer distribution in a three-phase hydrocracking process of FT wax have been presented and discussed. The influence of the operating conditions and the wax conversion on the isomer amount in the C_{23-} fraction has been pointed out with a particular attention to mono-branched and multi-branched isomer distribution. These experimental data allow a better understanding of the degree of isomerisation and the extent of both isomerisation and cracking reactions in the fuel cut. The distinction between mono-branched and multi-branched isomers is very important since the number of side chains (along with the total isomer amount) has a deep influence on both cold flow properties and cetane number of the produced synthetic fuel.

Moreover the analysis of detailed experimental data able to distinguish between mono-branched and multi-branched isomers can help in developing and validate kinetic models for the FT wax hydrocracking process more detailed with respect to those already developed [29–34] for a complex mixture of industrial interest.

References

[1] http://www.dieselnet.com/.

[2] V. Calemma, C. Gambaro, W.O. Parker Jr., R. Carbone, R. Giardino, P. Scorletti, Middle distillates from hydrocracking of FT waxes: composition, characteristics and emission properties, Catal. Today 149 (2010) 40–46.

[3] T.A. Alleman, R.L. McCormick, Fischer–Tropsch diesel fuels-properties and exhaust emission: a literature review, in: 2003 SAE World Congress, Detroit, MI, USA, March 3–6, 2003, SAE Technical Paper no. 2003-01-0763.

[4] T. Takeshita, K. Yamaji, Important roles of Fischer–Tropsch synfuels in the global energy future, Energy Policy 36 (2008) 2773–2784.

[5] A. Faaij, Modern biomass conversion technologies, Mitig. Adaptation Strateg. Glob. Change 11 (2006) 343–375.

[6] H. Boerrigter, H.P. Calis, D.J. Slort, H. Bodenstaff, A.J. Kaandorp, H. den Uil, L.P.L.M. Rabou, Gas Cleaning for Integrated Biomass Gasification (BG) and Fischer–Tropsch (FT) Systems, Energy Research Centre of The Netherlands, 2004, report no. ECN-C-04-056.

[7] H. Boerrigter, Economy of Biomass-to-Liquids (BTL) Plants: An Engineering Assessment, Energy Research Centre of The Netherlands, 2006, report no. ECN-C-06-019.

[8] R.W.R. Zwart, H. Boerrigter, High efficiency co-production of synthetic natural gas (SNG) and Fischer–Tropsch (FT) transportation fuels from biomass, Energy Fuels 19 (2005) 591–597.

[9] C.N. Hamelinck, A.P.C. Faaij, H. den Uil, H. Boerrigter, Production of FT transportation fuels from biomass; technical options, process analysis and optimisation, and development potential, Energy 29 (2004) 1743–1771.

[10] G.W Huber, S. Iborra, A. Corma, Synthesis of transportation fuels from biomass: chemistry, catalysts, and engineering, Chem. Rev. 106 (2006) 4044–4098.

[11] K.D. Maher, D.C. Bressler, Pyrolysis of triglyceride materials for the production of renewable fuels and chemicals, Bioresour. Technol. 98 (2007) 2351–2368.

[12] M.K. Bahng, C. Mukarakate, D.J. Robichaud, M.R. Nimlos, Current technologies for analysis of biomass thermochemical processing: a review, Anal. Chim. Acta 651 (2009) 117–138.

[13] M. Balat, M. Balat, E. Kırtay, H. Balat, Main routes for the thermo-conversion of biomass into fuels and chemicals. Part 2: gasification systems, Energy Convers. Manage. 50 (2009) 3158–3168.

[14] R.B. Anderson, The Fischer–Tropsch Synthesis, Academic Press, New York, 1984.

[15] V. Calemma, S. Guanziroli, S. Pavoni, R. Giardino, Process for the production of paraffinic middle distillates, European Patent 1404783 (B1) (2005).

[16] J.P. Collins, J.J.H.M. Font Freide, B. Nay, A history of Fischer–Tropsch wax upgrading at BP-from catalyst screening studies to full scale demonstration in Alaska, J. Nat. Gas Chem. 15 (2006) 1–10.

[17] M.E. Dry, The Fischer–Tropsch process: 1950–2000, Catal. Today 71 (2002) 227–241.

[18] V. Calemma, S. Peratello, S. Pavoni, G. Clerici, C. Perego, Hydroconversion of a mixture of long chain n-paraffins to middle distillate: effect of the operating parameters and products properties, in: E. Iglesia, J.J. Spivey, T.H. Fleish (Eds.), Natural Gas Conversion VI, Stud. Surf. Sci. Catal., vol. 136, Elsevier, Amsterdam, 2001, pp. 307–312.

[19] S.T. Sie, M.M.G. Senden, H.M.H. Van Wechem, Conversion of natural gas to transportation fuels via the Shell Middle Distillate Synthesis process (SMDS), Catal. Today 8 (1991) 371–394.

[20] L.P. Dancuart, R. de Haan, A. de Klerk, Processing of primary Fischer–Tropsch products, in: A. Steynberg, M. Dry (Eds.), Fischer–Tropsch Technology, Stud. Surf. Sci. Catal., vol. 152, Elsevier, Amsterdam, 2004, pp. 482–532.

[21] D. Leckel, M. Liwanga-Ehumbu, Diesel-selective hydrocracking of an iron-based Fischer–Tropsch wax fraction (C_{15}–C_{45}) using a MoO_3-modified noble metal catalyst, Energy Fuels 20 (2006) 2330–2336.

[22] G.R.B. Germaine, D.J. Wedlock, Process to prepare a waxy raffinate, United States Patent Application 20,040,099,571 (2004).

[23] T.G. Kaufmann, A. Kaldor, G.F. Stuntz, M.C. Kerby, L.L. Ansell, Catalysis science and technology for cleaner transportation fuels, Catal. Today 62 (2000) 77–90.

[24] D.J. O'Rear, Distillate fuel blends from Fischer Tropsch products with improved seal swell properties, United States Patent 6,890,423 (2005).

[25] J. Weitkamp, Isomerization of long-chain n-alkanes on a Pt/CaY zeolite catalyst, Ind. Eng. Chem. Prod. Res. Dev. 21 (1982) 550–558.

[26] M.J. Murphy, J.D. Taylor, R.L. McCormick, Compendium of Experimental Cetane Number Data, National Renewable Energy Laboratory, 2004, report no. NREL/SR-540-36805.

[27] V. Calemma, S. Correra, C. Perego, P. Pollesel, L. Pellegrini, Hydroconversion of Fischer–Tropsch waxes: assessment of the operating conditions effect by factorial design experiments, Catal. Today 106 (2005) 282–287.

[28] C. Perego, S. Peratello, Experimental methods in catalytic kinetics, Catal. Today 52 (1999) 133–145.

[29] L.A. Pellegrini, S. Gamba, V. Calemma, S. Bonomi, Modelling of hydrocracking with vapour–liquid equilibrium, Chem. Eng. Sci. 63 (2008) 4285–4291.

[30] L. Pellegrini, S. Locatelli, S. Rasella, S. Bonomi, V. Calemma, Modeling of Fischer–Tropsch products hydrocracking, Chem. Eng. Sci. 59 (2004) 4781–4787.

[31] L. Pellegrini, S. Bonomi, S. Gamba, V. Calemma, D. Molinari, The "all components hydrocracking model", Chem. Eng. Sci. 62 (2007) 5013–5020.

[32] L.A. Pellegrini, S. Gamba, V. Calemma, S. Bonomi, Hydrocracking reactor model with vapor/liquid equilibrium, in: 2007 AIChE Annual Meeting Conference Proceedings, AIChE Annual Meeting, November 4–9, 2007, Salt Lake City, UT, USA, AIChE, New York, 2007, paper 427g.

[33] S. Gamba, L.A. Pellegrini, V. Calemma, C. Gambaro, Introduction of a breakage probability function in the hydrocracking reactor model, Ind. Eng. Chem. Res. 48 (2009) 5656–5665.

[34] L.A. Pellegrini, S. Gamba, Hydrocracking of Fischer–Tropsch waxes: thermodynamic and kinetic aspects, Prepr. Am. Chem. Soc., Div. Pet. Chem. 54 (2) (2009) 82–85.

[35] S. Gamba, G.S. Soave, L.A. Pellegrini, Use of normal boiling point correlations for predicting critical parameters of paraffins for vapour–liquid equilibrium calculations with the SRK equation of state, Fluid Phase Equilib. 276 (2009) 133–141.

[36] I. Rossetti, C. Gambaro, V. Calemma, Hydrocracking of long chain linear paraffins, Chem. Eng. J. 154 (2009) 295–301.

[37] J.W. Thybaut, C.S. Laxmi Narasimhan, G.B. Marin, Bridging the gap between liquid and vapor phase hydrocracking, Catal. Today 111 (2006) 94–102.

[38] M.A. Baltanas, H. Vansina, G.F. Froment, Hydroisomerization and hydrocracking. 5. Kinetic analysis of rate data for n-octane, Ind. Eng. Chem. Prod. Res. Dev. 22 (1983) 531–539.

[39] M.T. Klein, G. Hou, Mechanistic kinetic modeling of heavy paraffin hydrocracking, in: C.S. Hsu, P.R. Robinson (Eds.), Practical Advances in Petroleum Processing, vol. 2, Springer Science and Business Media Inc., New York, 2006, pp. 187–204.

[40] J.A. Martens, P.A. Jacobs, J. Weitkamp, Attempts to rationalize the distribution of hydrocracked products. I. Qualitative description of the primary hydrocracking modes of long chain paraffins in open zeolites, Appl. Catal. 20 (1986) 239–281.

[41] J.A. Martens, P.A. Jacobs, J. Weitkamp, Attempts to rationalize the distribution of hydrocracked products. II. Relative rates of primary hydrocracking modes of long chain paraffins in open zeolites, Appl. Catal. 20 (1986) 283–303.

[42] L.A. Pellegrini, S. Gamba, S. Bonomi, V. Calemma, Equilibrium constants for isomerization of n-paraffins, Ind. Eng. Chem. Res. 46 (2007) 5446–5452.